Copper(II) Coordination Compounds with Bis(imidazol-2-yl)methylamine and Bis(imidazol-2-yl)methylaminomethane in Relation to Bis(imidazol-2-yl)methylamine-Modified Poly(glycidyl methacrylate) Polymers and Other Bis(imidazol-2-yl)-Containing Ligands

G. J. Anthony A. Koolhaas, Petronella M. van Berkel, Saskia C. van der Slot, Guillermo Mendoza-Diaz,† Willem L. Driessen,* and Jan Reedijk

Gorlaeus Laboratories, Leiden Institute of Chemistry, Leiden University, P.O. Box 9502, 2300 RA Leiden, The Netherlands

Huub Kooijman, Nora Veldman, and Anthony L. Spek

Department of Crystal and Structural Chemistry, Bijvoet Center for Biomolecular Research, Utrecht University, Padualaan 8, 3584 CH Utrecht, The Netherlands

Received October 25, 1995[⊗]

The synthesis, spectroscopy, and structure of three Cu(II) coordination compounds of the ligands bis(imidazol-2-yl)methylaminomethane (bimam) and bis(imidazol-2-yl)methylamine (bima) are described. The ligands bimam and bima both coordinate to Cu(II) ions in a didentate fashion. In all three complexes the copper(II) ions are coordinated in a distorted octahedral geometry. In $[Cu(Hbimam)Cl_3]_2(H_2O)_2$ and $[Cu(Hbima)Cl_3]_2(H_2O)_2$ each Cu(II) ion is coordinated by two imidazole nitrogens and four chloride anions. The two mononuclear units are connected by two asymmetric chloride bridges. In $[Cu(Hbimam)_2Cl_2]Cl_2(H_2O)_2$ the Cu(II) ion is coordinated by four imidazole nitrogens and two chloride anions. In the present complexes the amine nitrogen donor of the ligand is hydronated and not coordinated to the Cu(II) ion. [(De)hydronated is the recommended IUPAC expression to indicate loss/addition of H^+.] In all three complexes strong hydrogen bonding is observed between the amine nitrogen donor(s) and the axial coordinated chloride(s). X-ray crystallographic parameters for the copper complexes are as follows: $[Cu(Hbimam)Cl_3]_2(H_2O)_2$, monoclinic, space group $P2_1/c$, $Z = 4$, $a = 12.6259(8)$ Å, $b = 8.3452(4)$ Å, $c = 15.9280(8)$ Å, $\beta = 124.458(5)°$, $V = 1383.80(15)$ Å^3, $R = 0.037$, $R_w = 0.047$ for 2792 reflections with $I > 2.5\sigma(I)$; Cu−N 2.0271(18) and 1.992(2) Å, Cu−Cl 2.2705(8), 2.2854(8) 2.9266(11), and 3.2212(12) Å. $[Cu(Hbimam)_2Cl_2]Cl_2(H_2O)_2$, monoclinic, space group $P2_1/c$, $Z = 4$, $a = 7.6507(5)$ Å, $b = 21.4241(13)$ Å, $c = 14.8152(12)$ Å, $\beta = 93.285(6)°$, $V = 2424.4(3)$ Å^3, $R = 0.0289$ for 4781 reflections with $I > 2\sigma(I)$, $wR2 = 0.0716$ for 5534 reflections; Cu−N 2.0201(15), 1.9970(15), 2.0082(15), and 2.0102(15) Å; Cu−Cl 2.9019(5) and 2.9064(5) Å. $[Cu(Hbima)Cl_3]_2(H_2O)_2$, monoclinic space group $P2_1/c$, $Z = 4$, $a = 12.549(2)$ Å, $b = 8.345(2)$ Å, $c = 16.630(4)$ Å, $\beta = 126.22(2)°$, $V = 1405.0(6)$ Å^3, $R = 0.077$ for 1774 reflections with $I > 2\sigma(I)$, $wR2 = 0.190$ for 3208 reflections; Cu−N 1.997(6) and 2.018(6) Å; Cu−Cl 2.284(2), 2.286(2), 2.970(3), and 2.9843(3) Å. The ligand bimam was also immobilized onto a solid support, poly(glycidyl methacrylate-*co*-trimethylolpropane trimethacrylate) (p(GMT)), yielding a very Cu(II)-selective chelating ion-exchange resin pGMT-bimam with high uptake capacity. The resin retains its high uptake capacity for Cu(II) even in the presence of 1,2-diaminoethane, 1,3-diaminopropane and 1,4-diaminobutane as competing ligands in solution. When tartrate is used as a competitor, even a positive effect on the Cu(II) uptake is observed. For Na_2H_2edta as competitor in solution, both a pH effect and a concentration effect were noticed; *i.e.*, with increasing pH and increasing molar ratios (Na_2H_2edta:Cu(II)) the Cu(II) uptake of the ion exchanger decreases rapidly. Comparative spectroscopic studies of the coordination compounds with bimam and bima in their relationship to chelation of Cu(II) ions on the ion-exchange resin pGMT-bimam, have shown that on the resin only 1:1 (Cu(II):bimam) complexes are formed.

Introduction

A unique feature of metalloproteins is their capability to discriminate between various metal ions which are present in their natural surroundings. The active site of a metalloprotein is built up in such a way that only a few specific metal ions fit in, thus making the metal ions an integral part of the active site. Both the architecture of the active site and the metal ion determine the specific function of the different metalloproteins.[1]

Copper ions, as centers of the active site of various metalloproteins, play an essential role in biological processes like electron transfer, oxidation, and dioxygen transport.[2] In copper proteins, the copper ions are coordinated by donor atoms of the side chains of amino acid residues. Except for the Cu(I) metallothioneins, all copper proteins studied so far contain one or more imidazole residues of histidine, bound to the copper

* Author to whom correspondence should be addressed.
† Present address: Universidad de Guanajuato, Facultad de Quimica, Noria Alta s/n, Guanajuato GTO 36050, Mexico.
⊗ Abstract published in *Advance ACS Abstracts,* May 1, 1996.

(1) (a) Solomon, E. I.; Hemming, B. L.; Root, D. E. In *Bioinorganic Chemistry of Copper*; Karlin K. D., Tyeklár Z., Eds.; Chapman & Hall: London, 1993. (b) *Metal Ions in Biological Systems*; Sigel, H., Ed.; Marcel Dekker Inc.: New York, 1981.
(2) Solomon, E. I.; Baldwin, M. J.; Lowery, M. D. *Chem. Rev.* **1992**, *92*, 521.

S0020-1669(95)01370-X CCC: $12.00

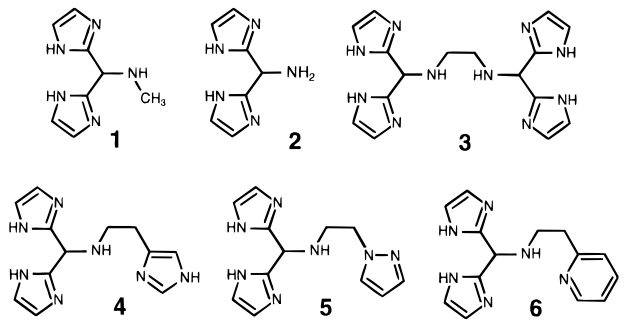

Figure 1. Schematic drawing of the ligands bimam (**1**), bima (**2**), Htidah (**3**), biib (**4**), bipab (**5**), and bipyb (**6**).

ion.[1] In the type-3 active site of dinuclear copper proteins like hemocyanin and tyrosinase, the only metal present is copper and each copper ion is bound by three imidazole nitrogens.[2,3]

Many model compounds have been synthesized which are aimed to mimic the active site of dinuclear copper proteins.[4] Because of the presence of histidine as a ligand to bind copper ions in almost all copper proteins,[1] copper complexes with the biologically relevant imidazolyl donors are increasingly studied as model compounds for copper protein active sites.[5] In the course of our research several new poly-imidazole ligands, *i.e.*, (Htidah) **3**, (biib) **4**, (bipab) **5**, and (bipyb) **6** (see Figure 1), have been designed and synthesized,[6−8] with the aim to model the type-3 active site. [Htidah (**3**) is 1,1,6,6-tetrakis(imidazol-2-yl)-2,5-diazahexane, biib (**4**) is 1,1-bis(imidazol-2-yl)-4-(imidazol-4(5)-yl)-2-azabutane, bipab (**5**) is 1,1-bis(imidazol-2-yl)-4-(pyrazole-1-yl)-2-azabutane, and bipyb (**6**) is 1,1-bis(imidazol-2-yl)-4-(pyridine-2-yl)-2-azabutane.] Various copper(II) coordination compounds have been synthesized with these ligands.[6−8] A general feature of these poly-imidazole ligands is that they all contain the same bis(imidazol-2-yl)-methylamine unit. To understand the coordination behavior of ligands with this specific unit, the binding properties of the ligands bis(imidazol-2-yl)methylaminomethane (bimam) and bis(imidazol-2-yl)methylamine (bima) (see Figure 1) have been investigated.[9−11]

Furthermore, synthetic analogues for copper protein active sites can be used in technical applications, *e.g.*, ion-exchange materials or catalysts.[12,13] By anchoring the designed ligands onto a solid support, systems with a high selectivity for copper and/or catalytic activity may be obtained.[14,15] As communicated earlier,[16] immobilization of the ligand bimam onto poly(glycidyl methacrylate-*co*-trimethylolpropane trimethacrylate) (pGMT) results in an ion-exchange resin (pGMT-bimam) (see Figure 2) with a high selectivity and a high uptake capacity in the pH range 1.1−6.0 for Cu^{2+} over Ni^{2+}, Co^{2+}, Zn^{2+}, and Cd^{2+}, as chloride salts in buffered solutions under competitive conditions.[16] Unfortunately, relatively little detailed information can be obtained about the coordination environment of metal-ion complexes in the heterogeneous phase. Therefore, coordination compounds with the ligands bimam and bima, obtained in the homogeneous phase, are used to provide more information about these resin-bound complexes.

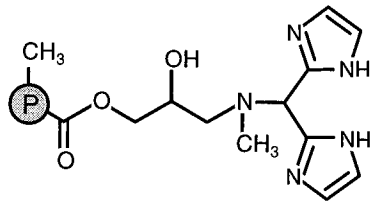

Figure 2. Schematic representation of the ion exchanger pGMT-bimam.

In the present paper relevant Cu(II) complexes with the ligands bimam and bima and chloride as the anion are presented and discussed in their relationship to the formation of multinuclear complexes with the poly-imidazole ligands Htidah, biib, bipab, and bipyb and to their chelation properties on the ion-exchange resin pGMT-bimam. Furthermore, the resin pGMT-bimam was also tested in the presence of competing chelating ligands in solution to determine whether the resin retains its initial high uptake capacity for Cu(II).

Experimental Section

Analysis and Spectroscopy. Elemental analyses (C, H, N) were performed by the Microanalytical Department of the Groningen University (The Netherlands). Metal analysis were carried out on a Perkin-Elmer 3100 atomic absorption (AAS) and flame emission spectrometer connected to a Perkin-Elmer AS-90 autosampler by using a nonlinear calibration method.

Fourier transform infrared spectra (4000−200 cm^{-1}) were recorded on a Bruker IFS 113V FT IR spectrophotometer connected to a Bruker IFS 113V data station, as KBr pellets. Solid-state electronic spectra (28000−5000 cm^{-1}) obtained by using the diffuse reflectance method with MgO or dried Zn(II)-loaded resins as a reference were recorded on a Perkin Elmer 330 spectrophotometer equipped with a data station.

X-band EPR spectra (powder or frozen solution) were recorded on a Jeol JES-RE2X electron spin resonance spectrometer equipped with a JEOL Esprit 330 data system at room temperature and 77 K with dpph as an internal reference. Variable temperature X-band powder EPR spectra were obtained on a Jeol JES-RE2X electron spin resonance spectrometer by using an ESR900 continuous-flow cryostat.

Starting Materials. Commercially available starting materials of sufficient purity were used without further treatment, unless stated otherwise. The metal solutions and buffer solutions used in the present study were prepared from analytical grade reagents. The ligands bimam and bima·3HCl were prepared as described by Joseph *et al.*[10] The pGMT polymer was prepared by radical-initiated suspension polymerization, using a mixture of glycidyl methacrylate (GMA) and trimethylolpropane trimethacrylate (TRIM) (1/1 v/v) with ethyl acetate as a porogen (monomer:porogen 1:2 v/v) as described by Verweij *et al.*[17] The BET surface area[18] of the starting pGMT polymer in the dry state is 110 m^2/g and the pore volume is 0.66 cm^3/g. The average

(3) (a) Magnus, K. A.; Ton−That, H.; Carpenter, J. *Chem. Rev.* **1994**, *94*, 727. (b) Magnus, K. A.; Hazes, B.; Ton−That, H; Bonaventura, C.; Bonaventura, J.; Hol, W. G. J. *Proteins* **1994**, *19*, 302.
(4) Kitajima, N.; Mora-oka, Y. *Chem. Rev.* **1994**, *94*, 737.
(5) (a) Wei, N.; Murthy, N. N.; Tyeklár, Z.; Karlin, K. D. *Inorg. Chem.* **1994**, *33*, 1177. (b) Sorrell, T. N.; Garrity, M. L.; Richards, J. L.; White, P. S. *Inorg. Chim. Acta* **1994**, *218*, 103. (c) Lynch, W. E.; Kurtz, D. M., Jr.; Wang, S.; Scott, R. A. *J. Am. Chem. Soc.* **1995** *116*, 11030. (d) Sorrell, T. N.; Allen, W. E.; White, P. S. *Inorg. Chem.* **1995**, *34*, 952.
(6) Koolhaas, G. J. A. A.; Driessen, W. L.; Reedijk, J.; Kooijman, H.; Spek, A. L. *J. Chem. Soc., Chem. Commun.* **1995**, 517.
(7) Koolhaas, G. J. A. A.; Driessen, W. L.; Reedijk, J.; van der Plas, J. L.; de Graaff, R. A. G.; Gatteschi, D.; Kooijman, H.; Spek, A. L. *Inorg. Chem.*, in press.
(8) Koolhaas, G. J. A. A.; Driessen, W. L.; van Koningsbruggen, P. J.; Reedijk, J.; Spek, A. L. *J. Chem. Soc. Dalton Trans* **1993**, 3803.
(9) Mendoza-Diaz, G.; Koolhaas, G. J. A. A.; Driessen, W. L.; Reedijk, J. *Acta Crystallogr.* **1995**, *C51*, 918.
(10) Joseph, M.; Leigh, T.; Swain, M. L. *Synthesis* **1977**, 459.
(11) Mulliez, E. *Tetrahedron Lett.* **1989**, *45*, 6169.
(12) Sahni, S. K.; Reedijk, J. *Coord. Chem. Rev.* **1984**, *59*, 1.
(13) Sherrington, D. C., Hodge, P., Eds. *Synthesis and Separations using Functional Polymers*; Wiley: London, 1988.
(14) Verweij, P. D.; van der Geest, J. S. N.; Driessen, W. L.; Reedijk, J.; Sherrington, D. C. *Reactive Polym.* **1992**, *18*, 191.
(15) van Berkel, P. M.; Verweij, P. D.; Driessen, W. L.; Reedijk, J; Sherrington, D. C. *Eur. Polym. J.* **1992**, *28*, 747.
(16) van Berkel, P. M.; Driessen, W. L.; Koolhaas, G. J. A. A.; Reedijk, J.; Sherrington, D. C. *J. Chem. Soc., Chem. Commun.* **1995**, 147.
(17) Verweij, P. D.; Sherrington, D. C. *J. Mater. Chem.* **1991**, *1*, 371.
(18) Brunauer, S.; Emmett, P. H.; Teller, E. *J. Am. Chem. Soc.* **1938**, *60*, 309.

Table 1. Crystallographic Data of the Coordination Compounds $[Cu(Hbimam)Cl_3]_2(H_2O)_2$ (**A**), $[Cu(Hbimam)_2Cl_2]Cl_2(H_2O)_2$ (**B**), and $[Cu(Hbima)Cl_3]_2(H_2O)_2$ (**C**)

	A	**B**	**C**
formula	$C_8H_{14}Cl_3CuN_5O$	$C_{16}H_{28}Cl_4CuN_{10}O_2$	$C_{14}H_{20}Cl_6Cu_2N_{10}$a
formula weight	366.14	597.82	334.09[a]
crystal system	monoclinic	monoclinic	monoclinic
space group	$P2_1/c$ (No. 14)	$P2_1/c$ (No. 14)	$P2_1/c$ (No. 14)
a, Å	12.6259(8)	7.6507(5)	12.549(2)
b, Å	8.3452(4)	21.4241(13)	8.345(2)
c, Å	15.9280(8)	14.8152(12)	16.630(4)
β, deg	124.458(5)	93.285(6)	126.22(2)
V, Å^3	1383.80(15)	2424.4(3)	1405.0(6)
Z	4	4	4
d_{calc}, g cm^{-3}	1.757	1.638	1.579[a]
μ_{calc}, cm^{-1}	21.6	13.8	21.1[a]
temp, K	298	150	150
radiatn, Å	(Mo Kα) 0.71073	(Mo Kα) 0.71073	(Mo Kα) 0.71073
R[b]	0.037	0.029	0.077
	$2792I > 2.5\sigma(I)$	$4781I > 2\sigma(I)$	$1774I > 2\sigma(I)$
R_w[c]	0.047		
wR2[d]		0.072	0.190

[a] Without disordered solvent contribution. [b] $R = \sum||F_o| - |F_c||/\sum|F_o|$. [c] $R_w = [\sum[w(||F_o| - |F_c||^2]/[w(F_o^2)]]^{1/2}$. [d] wR2 $= [\sum[w(F_o^2 - F_c^2)^2]/\sum[w(F_o^2)^2]]^{1/2}$.

particle diameter of the polymer beads is 375−500 μm. The immobilization of the ligand bimam onto pGMT and characterization of the resin pGMT-bimam has been described elsewhere.[16] The degree of conversion of epoxy groups after reaction with bimam was calculated from elemental analysis (C, H, N) to be 0.19, corresponding to a ligand concentration of 0.55 mmol/g of resin.

Synthesis of the Coordination Compounds. The coordination compounds $[Cu(Hbimam)Cl_3]_2(H_2O)_2$ and $[Cu(Hbimam)_2Cl_2]Cl_2(H_2O)_2$ were prepared by dissolving $CuCl_2 \cdot 2H_2O$ (respectively 1 and 3 mmol) in 10 mL of hot ethanol (96%) and adding this solution to a solution of the ligand (1 mmol in 10 mL of ethanol (96%)). The solution was filtered and after 2 days the crystalline products were collected by filtration, washed with ethanol, and dried in air. The complex $[Cu(Hbima)Cl_3]_2(H_2O)_2$ was prepared by dissolving $Cu(ClO_4)_2 \cdot 6H_2O$ (1 mmol) in 5 mL of ethanol/water and adding this solution to a solution of the trihydrochloride salt of the ligand (1 mmol) in 10 mL of ethanol/water (50/50). The solution was warmed to 40 °C and filtered. After 3 weeks the crystalline product was collected by filtration, washed with ethanol and dried in air. $[Cu(Hbimam)Cl_3]_2(H_2O)_2$: (Found: C, 26.38%; H, 3.87%; N, 19.01%. Calcd: C, 26.24%; H, 3.85%; N, 19.13%). $[Cu(Hbimam)_2Cl_2]Cl_2(H_2O)_2$. (Found: C, 31.92%; H, 4.87%; N, 22.61%. Calcd: C, 32.15%; H, 4.72%; N, 23.43%. $[Cu(Hbima)Cl_3]_2(H_2O)_2$. (Found: C, 25.66%; H, 3.09%; N, 20.96%. Calcd: C, 25.17 %; H, 3.02%; N, 20.96%).

Crystal Structure Determination of $[Cu(Hbimam)Cl_3]_2(H_2O))_2$ (A), $[Cu(Hbimam)_2Cl_2]Cl_2(H_2O)_2$ (B), and $[Cu(Hbima)Cl_3]_2(H_2O)_2$ (C). Crystals suitable for X-ray structure determination were either sealed in a Lindeman glass capillary (**A**) or glued to the top of a capillary (**B** and **C**) and transferred to an Enraf-Nonius CAD4-T diffractometer with a rotating anode. Accurate unit-cell parameters and an orientation matrix were determined by least-squares refinement of the setting angles of 25 well-centered reflections (SET4) in the ranges $11.32° < \theta < 14.11°$, $11.21° < \theta < 13.90°$, and $9.90° < \theta < 14.04°$ (for **A**, **B**, and **C**, respectively). Reduced-cell calculations did not indicate higher lattice symmetry.[19] Crystal data and details on data collection are collected in Table 1. Data were collected in ω scan mode (**A**) or $\omega/2\theta$ (**B** and **C**). The scan angle was $\Delta\omega = a + 0.35 \tan\theta°$, with $a = 0.80$, 0.50 and 0.90 For **A**, **B** and **C** respectively. Intensity data were collected up to $\theta = 27.50°$. Total data of 7097, 9689, and 3357 reflections were collected of which 3188, 5534 and 3215 were indipendent (R_{int} = 0.032, 0.024, and 0.066) for **A**, **B**, and **C**, respectively. Data were corrected for *Lp* effects and for the linear decay of three periodically measured reference reflections during X-ray exposure time. For compound **A** the standard deviations of the intensities as obtained by counting statistics were increased according to an analysis of the excess variance of the reference reflections $\sigma^2(I) = \sigma^2_{cs}(I) + (0.04I)$.[2,20] An empirical absorption correction (DIFABS[21]) was applied for compounds **A** and **B**, correction ranges 0.0675−1.436 and 0.889−1.081, respectively; a numerical absorption correction (ABSORB[22]) was applied for **C**, correction range 1.238−1.563.

The structures were solved by automated Patterson methods and subsequent difference Fourier techniques (DIRDIF-92[23]). Refinement on F was carried out by full matrix least-squares techniques (SHELX 76[24]) for compound **A**. Compounds **B** and **C** were refined on F^2 using full-matrix least-squares techniques (SHELXL 93[25]); no observance criterium was applied during refinement. Hydrogen atoms (including the primary amine hydrogen atoms of compound **C**) were included in the refinement on calculated positions riding on their carrier atoms, except for the secondary amine and water hydrogen atoms, which were located on a difference fourier map and subsequently included in the refinement.

After anisotropic refinement of the non-hydrogen atoms of **C** and introduction of the hydrogen atoms at expected positions, a difference Fourier revealed a number of residual density peaks (approximately 3 e Å^{-3}) in two symmetry-related cavities, located at $x = {}^1/_2$, $y = 0$, $z = {}^1/_2$, $x = {}^1/_2$, $y = {}^1/_2$, $z = 0$. No discrete solvent model could be be refined. The BYPASS procedure,[26] as implemented in the program PLATON,[27] was used to take this electron density into account. A total number of 48 electrons were found in each of the two cavities, which had a volume of 137.3 Å^3 each. The cavities are probably occupied by solvent molecules. Since the boundary of the disordered solvent region is difficult to define, due to hydrogen bonding of the amine and imidazole functions toward the disordered solvent, it is not possible to assess the correct occupancy of the cavities. The refined model remained poor, as is shown in the unusual anisotropic thermal parameters of N(13).

All non-hydrogen atoms were refined with anisotropic thermal parameters. The hydrogen atoms of **A** were refined with an overall isotropic thermal parameter with a value of 0.085(4) Å^2. The hydrogen atoms of the other compounds were included in the refinement with a

(19) Spek, A. L. *J. Appl. Crystallogr.* **1988**, *21*, 578.
(20) McCandlish, L. E.; Stout, G. H.; Andrews, L. C. *Acta Crystallogr.* **1975**, *A31*, 245.
(21) Walker, N.; Stewart, D. *Acta Crystallogr.* **1983**, *A39*, 158.
(22) Spek, A. L. *ABSORB Program for absorption correction*; Utrecht University: The Netherlands, 1983; ECM Abstract Book, p 283.
(23) Beurskens, P. T., Admiraal, G.; Beurskens, G.; Bosman, W. P.; Garcia-Granda, S.; Gould, R. O.; Smits, J. M. M.; Smykalla, C. *The DIRDIF program system*; Technical Report of the Crystallography Laboratory, University of Nijmegen: The Netherlands, 1992.
(24) Sheldrick, G. M. SHELX76. *Crystal Structure Analysis Package*; University of Cambridge: Cambridge, U. K., 1976.
(25) Sheldrick, G. M. SHELX93. *Program for crystal structure refinement*; University of Göttingen: Göttingen, Germany, 1993.
(26) van der Sluis, P.; Spek, A. L. *Acta Crystallogr.* **1990**, *A46*, 194.
(27) Spek, A. L. *Acta Crystallogr.* **1990**, *A46*, C34.

fixed isotropic thermal parameter related to the value of the equivalent isotropic thermal parameter of their carrier atoms by a factor of 1.5 for the methyl and amine hydrogen atoms and 1.2 for the other hydrogen atoms.

For **A** convergence was reached at $R = 0.037$, $w = 1/[\sigma^2(F) + 0.000133F^2]$, $R_w = 0.047$, S = 0.92 for 174 parameters and 2792 reflections with $I > 2.5\sigma(I)$. No residual density was found outside −0.75 and 0.56 e Å^{-3}. For **B** convergence was reached at $wR2 = 0.072$, $w^{-1} = \sigma^2(F^2) + (0.0667P)^2 + 1.30P$, where $P = (\mathrm{Max}(F_o2, 0) + 2F_c2)/3$, $R = 0.029$ [for 2415 $I > 2\sigma(I)$], S = 1.03 for 324 parameters. No residual density was found outside −0.43 and 0.40 e Å^{-3}. For **C** convergence was reached at $wR2 = 0.190$, $w^{-1} = \sigma^2(F^2) + (0.08P)^2$, $R = 0.077$ [for 1774 $I > 2\sigma(I)$], S = 1.13 for 146 parameters. No residual density outside −1.15 and 1.19 e Å^{-3} (near Cu) was found.

Neutral atom scattering factors and anomalous dispersion corrections were taken from the International Tables for Crystallography[28] for compound **B** and **C**. For compond **A** neutral atom scattering factors were taken from Cromer and Mann;[29] anomalous dispersion corrections were from Cromer and Liberman.[30] Geometrical calculations were performed with PLATON.[27]

Batch Metal-Uptake Experiments. Batch metal-uptake experiments with the ion-exchange resin pGMT-bimam and competing ligands (L_c) in solution were performed by using 0.011 M $CuCl_2$ solutions, buffer solutions (B) of 0.6 M (NaOAc/HOAc, pH 2.9−6.2), and 0.011 M L_c solutions. The competing ligands tested were 1,2-diaminoethane, 1,3-diaminopropane, 1,4-diaminobutane, tartrate, and Na_2H_2edta. All experiments were performed in polyethylene bottles mounted on a shaker at 25 °C. The capacity for Cu(II) was determined as a function of pH in the presence of competing ligands in solution. Batches of 0.2 g of resin (containing 0.11 mmol of immobilized ligand (L_i)) were used, together with a mixture of 10 mL of $CuCl_2$ solution and 40 mL of B, or 35 mL of B and 5 ml of L_c, or 30 mL of B and 10 mL of L_c, or 25 mL of B and 15 mL L_c, or 30 mL of B and 10 mL of L_c (0.055 M). In this way the following molar ratios were obtained L_i:L_c:$CuCl_2$ is 1:0:1, 1:0.5:1, 1:1:1, 1:1.5:1, and 1:5:1. After a shaking time of 48 h, the samples were filtered, washed subsequently with water, ethanol, and diethyl ether, and dried *in vacuo* at 50 °C.

Samples for Cu(II) analysis were prepared by heating 0.1 g of the loaded samples with concentrated H_2SO_4 and subsequently with concentrated HNO_3 until clear solutions were obtained. The Cu(II) contents of these solutions were measured by AAS spectroscopy using a previously determined nonlinear calibration curve.

Spectroscopic Characterization of the Loaded Resins. To obtain information about the coordination environment of the metal ions when bound to the resin, ligand field (LF) spectra in the visible and near-infrared region (vis−NIR) and EPR spectra of several loaded resins were recorded. Batches of about 0.2 g of pGMT-bimam were treated with aqueous solutions of 0.16 M MCl_2 (where M is Cu(II), Ni(II), and Co(II)) and NaCl/HCl (pH 0.9−2.3) and NaOAc/HOAc (pH 2.5−6.0) buffer solutions ($I = 0.6$ M). Batches of 0.2 g of resin were used, together with a mixture of 25 mL of metal solution and 25 mL of buffer. After a shaking time of 48 h, the samples were filtered, washed subsequently with water, ethanol, and diethyl ether, and dried *in vacuo* at 50 °C. For the uptake of Cu(II) at pH > 5 a lower Cu(II) concentration (10 mL of Cu^{2+} solution (0.16 M) and 40 mL of buffer) was used to prevent precipitation of Cu(II) hydroxides. To determine whether or not the additional competing ligands in solution are involved in the coordination environment around the Cu(II) ion, samples of resins loaded with Cu(II) in the presence of these competing ligands were prepared at different pH values as described for the batch metal-uptake capacity experiments. The LF spectra were recorded in the 28000−5000 cm^{-1} range in the diffuse reflectance mode with dried Zn(II)-loaded samples as reference substances. EPR spectra were recorded at room temperature and 77 K. A variable temperature EPR spectrum was obtained of a Cu(II)-loaded resin at pH 1.7.

Table 2. Selected Bond Lengths (Å) Involving Non-Hydrogen Atoms and Selected Bond Angles (deg) in $[Cu(Hbimam)Cl_3]_2(H_2O)_2$ (**A**), $[Cu(Hbimam)_2Cl_2]Cl_2(H_2O)_2$ (**B**), and $[Cu(Hbima)Cl_3]_2(H_2O)_2$ (**C**)

Complex **A**

Cu(1)−Cl(1)	2.2705(8)	Cu(1)−Cl(3)	2.9266(11)
Cu(1)−Cl(2)	2.2854(8)	Cu(1)−Cl(1)[a]	3.2212(12)
Cu(1)−N(13)	2.0271(18)	Cu(1)−Cu(1)[a]	4.0142(6)
Cu(1)−N(23)	1.992(2)		

Cl(1)−Cu(1)−Cl(2)	92.07(3)	Cl(2)−Cu(1)−N(23)	89.00(7)
Cl(1)−Cu(1)−N(13)	92.84(6)	N(13)−Cu(1)−N(23)	87.44(9)
Cl(1)−Cu(1)−N(23)	168.38(9)	Cu(1)−Cl(1)−Cu(1)[a]	92.28(4)
Cl(2)−Cu(1)−N(13)	172.08(8)		

Complex **B**

Cu(1)−Cl(1)	2.9019(5)	Cu(1)−N(23)	1.9970(15)
Cu(1)−Cl(2)	2.9064(5)	Cu(1)−N(33)	2.0082(15)
Cu(1)−N(13)	2.0201(15)	Cu(1)−N(43)	2.0102(15)

Cl(1)−Cu(1)−Cl(2)	171.75(1)	Cl(2)−Cu(1)−N(43)	91.13(4)
Cl(1)−Cu(1)−N(13)	89.15(4)	N(13)−Cu(1)−N(23)	86.41(6)
Cl(1)−Cu(1)−N(23)	87.47(4)	N(13)−Cu(1)−N(33)	95.58(6)
Cl(1)−Cu(1)−N(33)	89.36(4)	N(13)−Cu(1)−N(43)	175.49(6)
Cl(1)−Cu(1)−N(43)	94.26(4)	N(23)−Cu(1)−N(33)	176.23(6)
Cl(2)−Cu(1)−N(13)	85.81(4)	N(23)−Cu(1)−N(43)	90.79(6)
Cl(2)−Cu(1)−N(23)	98.71(4)	N(33)−Cu(1)−N(43)	87.42(6)
Cl(2)−Cu(1)−N(33)	84.64(4)		

Complex **C**

Cu(1)−Cl(2)	2.286(2)	Cu(1)−Cl(3)	2.970(3)
Cu(1)−Cl(1)	2.284(2)	Cu(1)−Cl(2)[a]	2.984(3)
Cu(1)−N(23)	2.018(6)	Cu(1)−Cu(1)[a]	3.8525(17)
Cu(1)−N(13)	1.997(6)		

Cl(2)−Cu(1)−Cl(1)	92.31(7)	Cl(1)−Cu(1)−N(13)	88.92(16)
Cl(2)−Cu(1)−N(23)	93.27(17)	N(23)−Cu(1)−N(13)	87.3(2)
Cl(2)−Cu(1)−N(13)	171.4(2))	Cu(1)−Cl(2)−Cu(1)[a]	92.98(9)
Cl(1)−Cu(1)−N(23)	167.2(2)		

[a] Denotes symmetry operation $(-x, -y, -z)$.

Table 3. Distances (D···A, Å) and Angles (D−H···A, deg) between the Parent Atoms of the Observed Intra- and Intermolecular Hydrogen Bonds in $[Cu(Hbimam)Cl_3]_2(H_2O)_2$ (**A**), $[Cu(Hbimam)_2Cl_2]Cl_2(H_2O)_2$ (**B**), and $[Cu(Hbima)Cl_3]_2(H_2O)_2$ (**C**)

Complex **A**

N(2)···Cl(3)	3.058(3)	169(4)	N(21)···O(2)[a]	2.834(3)	153.5(4)
N(2)···Cl(3)[a]	3.120(3)	149(4)	O(2)···Cl(3)	3.367(7)	155.9(6)
N(11)···Cl(1)[b]	3.266(3)	145.7(3)	O(2)···Cl(3)[c]	3.504(5)	145.4(8)

Complex **B**

N(12)···Cl(2)	2.999(2)	174(2)	N(32)···Cl(3)[d]	3.056(2)	162(2)
N(32)···Cl(1)	3.045(2)	168(2)	N(41)···Cl(1)[d]	3.126(2)	156.8(2)
N(11)···Cl(2)[a]	3.119(2)	141.2(2)	O(5)···Cl(3)[e]	3.104(2)	168(3)
N(12)···Cl(1)[b]	3.156(2)	142(2)	O(5)···Cl(4)[f]	3.020(2)	155(2)
N(12)···Cl(3)[b]	3.277(2)	118.7(18)	O(6)···O(5)	2.804(2)	179(3)
N(21)···O(5)[b]	2.762(2)	173.7(2)	O(6)···Cl(3)	3.242(2)	163(3)
N(31)···Cl(4)[c]	3.123(2)	155.1(2)			

Complex **C**

N(2)···Cl(3)	3.128(7)	156(3)	
N(2)···Cl(3)[a]	3.125(7)	135(5)	
N(21)···Cl(2)[b]	3.237(6)	153.7(7)	

[a] $(1-x, {}^1/_2+y, {}^1/_2-z)$. [b] $(x, 1+y, z)$. [c] $(1-x, -y, -z)$. [d] $(1+x, y, z)$. [e] $(x, {}^1/_2-y, -{}^1/_2+z)$. [f] $(-x, -{}^1/_2+y, {}^1/_2-z)$. [g] $(-1+x, y, z)$. [h] $(1-x, -y, 1-z)$. [i] $(x, {}^1/_2-y, {}^1/_2+z)$.

Results and Discussion

General. Bond distances, bond angles, and hydrogen bond distances of the three complexes are listed in Tables 2 and 3. PLUTON[31] projections of $[Cu(Hbimam)Cl_3]_2(H_2O)_2$ (**A**) and $[Cu(Hbimam)_2Cl_2]Cl_2(H_2O)_2$ (**B**) are depicted in Figures 3 and 4. Figure 5 shows the molecular structure and intermolecular

(28) Wilson, A. J. C., Ed. *International tables for X-ray Crystallography*; Kluwer Academic Publishers: Dordrecht, The Netherlands, 1992; Vol. C.
(29) Cromer, D. T.; Mann, J. B. *Acta Crystallogr.* **1968**, *A24*, 321.
(30) Cromer, D. T.; Liberman, D. *J. Chem. Phys.* **1970**, 53, 1891.
(31) Spek, A. L. *PLUTON Molecular graphics program*; Utrecht University: The Netherlands, 1995.

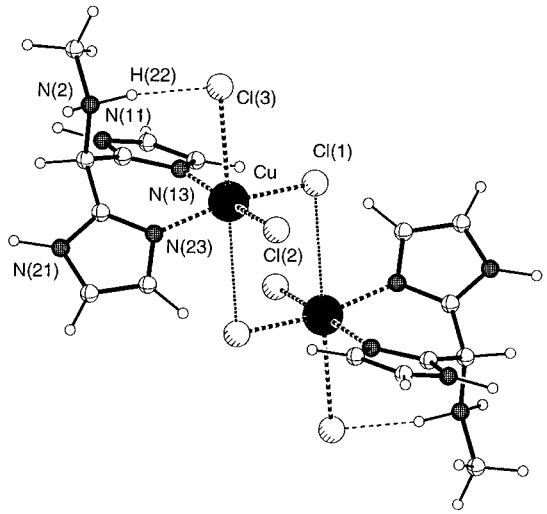

Figure 3. PLUTON[31] projection of the complex $[Cu(Hbimam)Cl_3]_2(H_2O)_2$ (**A**). Lattice water molecules are omitted for clarity.

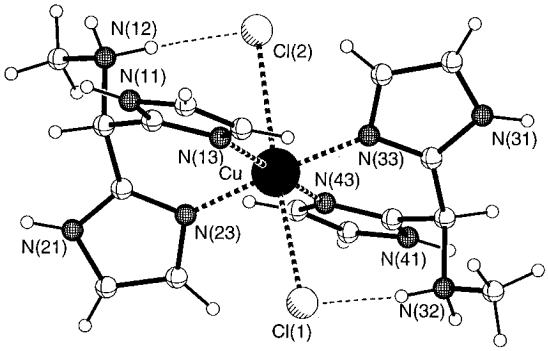

Figure 4. PLUTON[31] projection of the complex $[Cu(Hbimam)_2Cl_2]Cl_2(H_2O)_2$ (**B**). Noncoordinated anions and lattice water molecules are omitted for clarity.

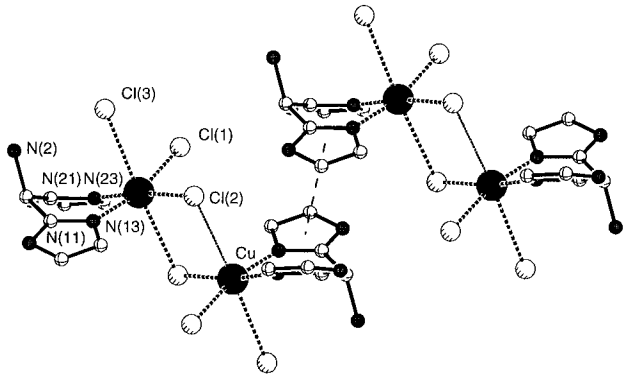

Figure 5. PLUTON[31] projection of the complex $[Cu(Hbima)Cl_3]_2(H_2O)_2$ (**C**) showing the intermolecular stacking (dashed line), hydrogen atoms are omitted for clarity

stacking interaction in $[Cu(Hbima)Cl_3]_2(H_2O)_2$ (**C**) (PLUTON[31] projection). A listing of the major spectroscopic data (ligand field and EPR) of the complexes is given in Table 4.

Description of the Crystal Structure of $[Cu(Hbimam)Cl_3]_2(H_2O)_2$ and $[Cu(Hbima)Cl_3]_2(H_2O)_2$. Both Cu(II) complexes crystallize in the monoclinic space group $P2_1/c$ with two dinuclear molecules in the unit cell. The asymmetric unit consists of one Cu(II) ion, a hydronated bimam ligand, and three chloride anions. The asymmetric unit of complex (**A**) contains one additional lattice water molecule. A difference Fourier of **C** revealed a number of residual density peaks, most probably from disordered solvent molecules, but no discrete solvent model could be refined.

Table 4. Ligand Field Absorption Bands (10^3 cm^{-1}) and EPR[a] Data of the Bimam and Bima Coordination Compounds

compound	LF bands	$g_\perp$, $g_\parallel$ (G)	$A_\parallel$ (G)	$A_{N\perp}$
$[Cu(Hbimam)Cl_3]_2(H_2O)_2$	13.6 (br)	2.07(1), 2.29(1)	162(2)	14.8(2)
$[Cu(Hbimam)_2Cl_2]Cl_2(H_2O)_2$	16.6	2.07(1), 2.25(1)	180(2)	15.0(2)
$[Cu(Hbima)Cl_3]_2(H_2O)_2$	13.6 (br)	2.07(1), 2.29(1)	162(2)	14.8(2)

[a] EPR spectra of the frozen solutions (MeOH/dmso, 50/50) at 77 K.

In each complex the Cu(II) ion is coordinated in a distorted octahedral geometry. In the equatorial plane the Cu(II) ion is bound to two imidazole nitrogens at distances of 2.0271(18) and 1.992(2) Å (**A**) and 1.997(6) and 2.018(6) Å (**C**) and to two chloride anions Cl(1) and Cl(2) at distances of 2.2705(8) and 2.2854(8) Å in **A** and 2.284(2) and 2.286(2) Å in **C**. Cl(1) in **A**, and Cl(2) in **C**, is bridging between the two copper ions and is axially coordinated to Cu(1)[a]. The Cu(1)[a]−Cl(1) distance is 3.2212(12) Å (**A**) and the Cu(1)[a]−Cl(2) distance is 2.984(3) Å (**C**), the bond angles Cu(1)−Cl−Cu(1)[a] are 92.28(4)° and 92.98(9)° for **A** and **C**, respectively. The two asymmetric chloride bridges separate the metals by 4.0142(6) and 3.8525(17) Å, for **A** and **C**, respectively. The other axial position of the Cu(II) ion is occupied by a single bonded chloride anion (Cu−Cl(3) is 2.9266(11) Å (**A**) and 2.970(3) Å (**C**)). The amine nitrogen donor (N(2)) in both complexes is hydronated and is not coordinated to the Cu(II) ion. H(22) which is bound to N(2) forms a hydrogen bond between N(2) and the apical chloride (Cl(3)). The different molecules are linked by intermolecular stacking of imidazole rings and by several hydrogen bonds. In each mononuclear unit one imidazole ring containing N(13) in **A** and N(23) in **C** stacks to the symmetry-related ($-x$, $1-y$, $-z$) imidazole ring in a neighboring molecule. The distance of the centroid of the ring to the least-squares plane through the symmetry-related ring is 3.539 Å for **A** and 3.592 Å for **C**. The dihedral angle between the two least-squares planes is 0.05° and 0.02° for **A** and **C**, respectively.

Description of the Crystal Structure of $[Cu(Hbimam)_2Cl_2]Cl_2(H_2O)_2$. The complex crystallizes in the monoclinic space group $P2_1/c$ with four molecules in the unit cell. The Cu(II) ion is coordinated by two ligands and two chloride anions in a distorted octahedral geometry. In the equatorial plane the Cu(II) ion is bound to four imidazole nitrogens at distances of 2.0201(15), 1.9970(15), 2.0082(15) and 2.0102(15) Å. Two chloride anions are coordinated axially to the Cu(II) ion at rather large distances of 2.9019(5) and 2.9064(5) Å. The amine nitrogen donors N(12) and N(32) of the two ligands are hydronated and are not coordinated to the Cu(II) ion. H(12b) and H(32b) form hydrogen bonds between N(12), N(32b), and the two axial coordinated chlorides. The different molecules are linked by intermolecular stacking of imidazole rings and by several hydrogen bonds. All observed hydrogen bonds are listed in Table 3. In each molecule one imidazole ring containing N(13) stacks to an imidazole ring containing N(43) in a neighbouring molecule (symm. $1+x$, y, z). The distance of the centroid of the first ring to the least-squares plane through the second ring is 3.512 Å. The dihedral angle between the two least-squares planes is 1.57°. The ring containing N(33) stacks to a symmetry related ring ($-x$, $-y$, $-z$) in a neighbouring molecule. The distance of the centroid of the ring to the least-squares plane through the symmetry-related ring is 3.347 Å. The dihedral angle between the two symmetry-related least-squares planes is 0.03°.

Comparison with Related Structures. The ligands bima and bimam both coordinate to copper(II) ions in a didentate fashion. In the copper(II) complex $[Cu(dpma)_2](ClO_4)_2$ of the

tridentate ligand di(2-pyridyl)aminomethane (dpma) reported by Comba and co-workers,[32] the copper(II) ion is coordinated by all three nitrogen donors of the ligand. Its crystal structure revealed that considerable steric strain resulted from this coordination, elongating one of the Cu−N(pyridine) bonds to as much as 2.536(6) Å. The ligand bites in bima and bimam are comparable to those in dpma. The smaller ring size and ring angles of imidazole compared to pyridine seriously hamper tridentate coordination in the complexes with the ligands bima and bimam.

Coordination chemistry studies with the ligand Htidah[8] also illustrate the inability of the bis(imidazol-2-yl)methylamine unit to encapsulate one copper(II) ion with all three nitrogen donor atoms. In the complex $[Cu_6(tidah)_2Cl_{10}(H_2O)_4](H_2O)_6$ one of the four imidazoles of each ligand is dehydronated, resulting in the formation of a hexanuclear cluster with a unique architecture[8]. By dehydronation of one imidazole group, all nitrogen donors of the two tidah ligands are able to coordinate to the six copper(II) ions, explaining the cluster formation. Dehydronation in bima and bimam would result in a dinuclear imidazolate bridged complex. Unfortunately crystallization of the complexes with the present ligands at high pH, which is required for the formation of an imidazolate, did not occur.

With the potential tetradentate ligands biib, bipab, and bipyb, dinuclear copper complexes were obtained[6,7] which are formed by the sharing of the bis(imidazole) units of two ligands by two Cu(II) ions. Due to the above-mentioned steric reasons, the three tetradentate ligands cannot coordinate to a single Cu(II) ion. Upon dimerization of the complexes all four nitrogen donors of the ligands are able to coordinate to the copper ions in a square planar fashion. This coordination behavior, *i.e.*, ligand sharing, is not observed in the three present complexes. By ligand sharing and the subsequent formation of a dinuclear complex all three nitrogen donors of the ligands bima and bimam would be able to coordinate to the copper ions, resulting in a more saturated coordination environment then observed in $[Cu(Hbimam)Cl_3]_2(H_2O)_2$ and $[Cu(Hbima)Cl_3]_2(H_2O)_2$.

A likely driving force for the formation of the present complexes and the hydronation of the amine nitrogen donors is the formation of an intramolecular hydrogen bond between the amine nitrogen donors and one of the axial coordinated chloride anions.

Spectroscopic Results. *EPR Spectra of the Coordination Complexes*. EPR spectra of the polycrystalline powders of the three complexes were recorded at room temperature and 77 K. The resolution of the spectra did not improve upon cooling from room temperature to 77 K. The three complexes all show axial $S = {}^1/_2$ spectra with $g_\perp = 2.07(3)$ and $g_{||} = 2.25(3)$; $A_{||}$ for $[Cu(Hbimam)_2Cl_2]Cl_2(H_2O)_2$ is 180(10) G, which is about the value expected for a copper(II) ion coordinated in the equatorial plane by four strong nitrogen donors.[33] No hyperfine splitting was observed for the compounds $[Cu(Hbimam)Cl_3]_2(H_2O)_2$ and $[Cu(Hbima)Cl_3]_2(H_2O)_2$. The $g_{||}$ values for the compounds $[Cu(Hbimam)Cl_3]_2(H_2O)_2$ and $[Cu(Hbima)Cl_3]_2(H_2O)_2$ are smaller than normally observed for a CuN_2Cl_3 or a CuN_2Cl_4 chromophore.[33]

Frozen-solution EPR spectra of the complexes recorded at 77 K in MeOH/dmso (50/50) show well-resolved axial $S = {}^1/_2$ spectra with superhyperfine splitting superimposed on the equatorial absorptions. The frozen-solution spectra of $[Cu(Hbimam)Cl_3]_2(H_2O)_2$ and $[Cu(Hbimam)_2Cl_2]Cl_2(H_2O)_2$ are depicted in Figure 6. The spectra of the compounds $[Cu(Hbimam)Cl_3]_2(H_2O)_2$ and $[Cu(Hbima)Cl_3]_2(H_2O)_2$ are identical, with $g_\perp = 2.07(1)$, $g_{||} = 2.29(1)$ and $A_{||} = 162(5)$ G. Five superhyperfine lines indicating the bonding of two nitrogen donors to the Cu(II) ion[33] with $A_{N\perp} = 14.8(5)$ G have been detected. The two chloro-bridged dinuclear Cu(II) complexes probably react in the MeOH−dmso solution to form mononuclear species in which, instead of the bridging chloride, a methanol or dmso donor atom is axially coordinated to the Cu(II) ion. The frozen solution spectrum of $[Cu(Hbimam)_2Cl_2]Cl_2(H_2O)_2$ in which $g_\perp = 2.07(1)$, $g_{||} = 2.25(1)$ and $A_{||} = 180(5)$ G shows nine superhyperfine lines with $A_{N\perp} = 15.0(5)$ G, in agreement with the bonding of four nitrogen donors to the Cu(II) ion.[33]

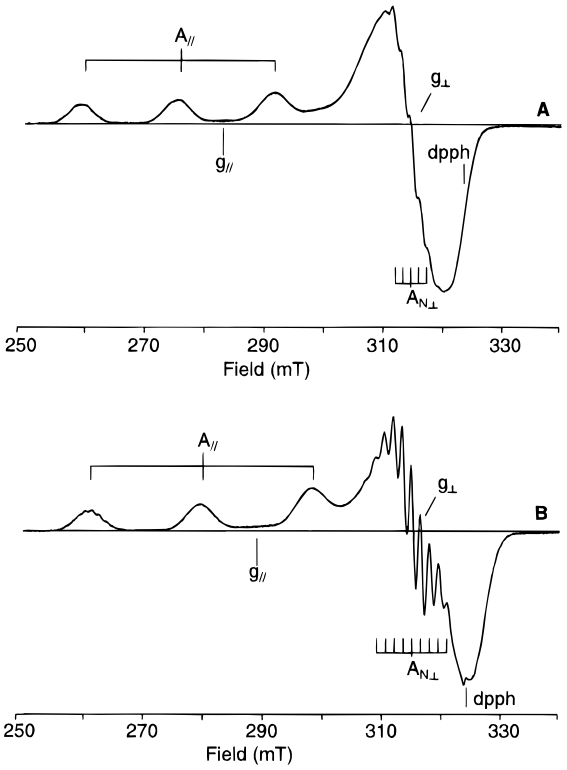

Figure 6. Frozen-solution EPR-spectra of $[Cu(Hbimam)Cl_3]_2(H_2O)_2$ and $[Cu(Hbimam)_2Cl_2]Cl_2(H_2O)_2$ recorded at 77 K in MeOH/dmso.

EPR of the Cu(II)-Loaded Resins. Solid-state EPR spectra of the Cu(II)-loaded resins obtained at pH = 1.7, 2.6, and 5.6 were recorded at room temperature and 77 K. Variable temperature EPR spectra in the range 298−4.2 K were recorded on the sample obtained at pH = 1.7. The resolution of the spectra did not improve upon cooling from room temperature to 77 or 4.2 K, and, unfortunately, no superhyperfine interactions were observed. The spectra of the three resins are almost identical with $g_\perp = 2.07(3)$, $g_{||} = 2.25(3)$ and $A_{||} = 160(10)$ G, strongly suggesting that the coordination environment of the copper(II) ion bound to the resin does not change in the pH range 1.7−5.6.

The $g_{||}$ and $A_{||}$ values of 2.25(3) and 160(10) G obtained from the solid-state EPR spectra of the Cu(II)-bound complexes on the resin resemble the $g_{//}$ and $A_{//}$ values (2.29(1) and 162(1)G) calculated from the frozen-solution spectra of $[Cu(Hbimam)Cl_3]_2(H_2O)_2$ and $[Cu(Hbima)Cl_3]_2(H_2O)_2$, which most probably indicates the formation of 1:1 complexes (Cu(II):bimam) on the polymer. It is therefore most likely that the coordination sphere of the Cu(II) ion on the polymer is formed by two imidazole

(32) Bernhard, P. V.; Comba, P.; Mahu-Rickenbach, A.; Stebler, S.; Steiner, S.; Varnagy K.; Zehnder, M. *Inorg. Chem.* **1992**, *31*, 4194.

(33) (a) Abragam A.; Bleaney, B. *Electron Paramagnetic Resonance of Transition Ions*; Clarendon Press: London, 1970; p 492. (b) Hathaway, B. J. *Comprehensive Coordination Chemistry*; Wilkinson, G.; Gillard, R. D.; McCleverty, J. A., Eds.; Pergamon Press: U. K., 1987; Vol. 5, p652.

nitrogen atoms of the ligand bimam, chloride ions (pH 1.7), acetate ions (pH 2.6 and 5.6), and/or some water molecules. This nicely explains the high uptake of Cu(II) at low pH, even though the aliphatic amine nitrogen donor of the immobilized bimam is most probably hydronated just as found in the three compounds obtained in the homogeneous phase. The formation of chloro-bridged dinuclear Cu(II) complexes is very unlikely, due to the restricted mobility of the immobilized ligands.

Solid-state EPR spectra obtained at room temperature of the Cu(II)-loaded resins (pH 2.9 and 5.9) in the presence of different molar ratios of Na_2H_2edta as competing ligand in solution (L_c), *i.e.*, L_i:L_c:$CuCl_2$ is 1:0:1, 1:0.5:1, and 1:1.5:1 (L_i is molar ratio of immobilized ligand), all show axial spectra with $g_\perp = 2.08(3)$, $g_\parallel = 2.26(3)$ and $A_\parallel = 165(10)$ G. The resolution of the spectra did not improve upon cooling to 77 K and no superhyperfine interactions were observed. The fact that there are hardly any differences between the $g_\parallel$ and $A_\parallel$ values obtained from the solid-state EPR spectra of Cu(II)-loaded samples in the presence or the absence of Na_2H_2edta most probably implies that Na_2H_2edta does not take part in the coordination environment of the Cu(II) ion on the polymer. Comparison of the EPR data ($g_\parallel$ and $A_\parallel$) of the frozen-solution spectra of $[Cu(Hbimam)Cl_3]_2(H_2O)_2$ and $[Cu(Hbima)Cl_3]_2(H_2O)_2$ with these data, again implies the formation of 1:1 complexes (Cu(II):bimam) in the heterogeneous phase.

The solid-state EPR spectra obtained at room temperature of the Cu(II)-loaded resins (pH 3.0 and 5.9) in the presence of different molar ratios of tartrate as competing ligand in solution all show axial spectra with $g_\perp = 2.08(3)$, $g_\parallel = 2.27(3)$, and $A_\parallel = 165(10)$ G. The presence or absence of tartrate as competing ligand in solution does not have an influence on the $g_\parallel$ and $A_\parallel$ values, *i.e.*, there are hardly any differences between the spectra. This was also the case for Na_2H_2edta as competing ligand in solution. It is very likely that tartrate does not take part in the coordination environment of the Cu(II) ion on the polymer. Comparison of the EPR data ($g_\parallel$ and $A_\parallel$) of the frozen-solution spectra of $[Cu(Hbimam)Cl_3]_2(H_2O)_2$ and $[Cu(Hbima)Cl_3]_2$-$(H_2O)_2$ with these data indicates the formation of 1:1 complexes (Cu(II):bimam) in the resin phase.

Ligand-Field Spectroscopy. The diffuse-reflectance spectra of $[Cu(Hbimam)Cl_3]_2(H_2O)_2$ and $[Cu(Hbima)Cl_3]_2(H_2O)_2$ in the vis−NIR region show one broad asymmetric band at 13.6×10^3 cm^{-1} in agreement with the CuN_2Cl_3 chromophore.[34,35] The spectrum of $[Cu(Hbimam)Cl_2]Cl_2(H_2O)_2$ shows a single sharp band at 16.6×10^3 cm^{-1}, which is usually observed for square planar or tetragonal coordinated copper(II) complexes.[34,35] The ligand-field spectra of the Cu(II) complexes formed on the resin pGMT-bimam at pH 2.6 and 5.6 show broad bands with an absorption maximum at respectively 13.6×10^3 and 13.9×10^3 cm^{-1}, and both show a small charge-transfer band around 30×10^3 cm^{-1}. Comparison of the ligand-field data of the Cu(II) complexes obtained in the homogeneous phase with these data also implies the formation of 1:1 complexes (Cu(II):bimam) on the polymer.

Besides ligand-field spectra of the Cu(II)-loaded resins, also ligand-field spectra of Ni(II)-loaded and Co(II)-loaded resins were obtained. The ligand-field spectrum of the ion-exchange resin pGMT-bimam loaded with Ni^{2+} at pH 5.6 shows electronic absorption bands at 24.9×10^3, 16.5×10^3, and 9.8×10^3 cm^{-1} which can be ascribed to a distorted octahedral coordination geometry around the Ni(II) ion.[34] Unfortunately, no reasonable ligand-field spectra could be obtained for pGMT-bimam loaded with Ni(II) ions at pH < 5.6 or of pGMT-bimam loaded with Co(II) ions in the pH range 0.9−6.0, due to the low concentrations of Ni(II) and Co(II) on the resin.

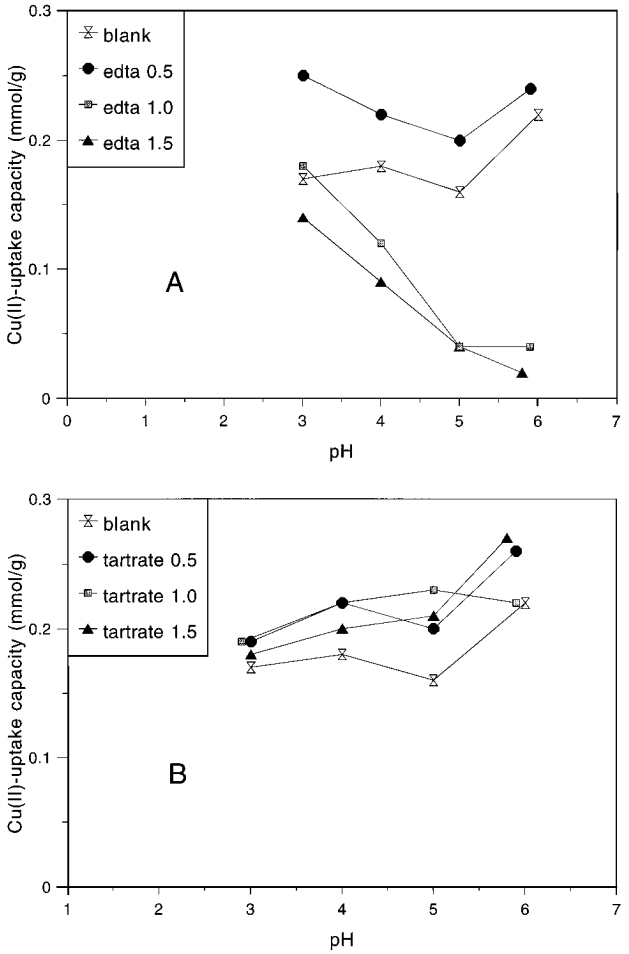

Figure 7. Capacity of pGMT-bimam for Cu^{2+} ions in the presence of different molar ratios of Na_2H_2edta (A) and tartrate (B) as a function of pH.

Batch Metal-Uptake Experiments. The results for the metal-uptake experiments with Na_2H_4edta and tartrate as competing ligands in solution are presented in Figure 7. The ligand concentration on pGMT-bimam is 0.55 mmol of bimam/g of resin. The maximum uptake capacity for Cu(II) in the absence of competing ligands is 0.22 mmol/g at pH 6.0. This would seem indicative of the presence of 1:2 complexes (Cu(II):bimam) on the polymer at pH 6.0. However, because of the rigidity of the polymer matrix, it is more likely that only 1:1 (Cu(II):bimam) complexes are formed[15]. Comparative spectroscopic studies, EPR, and ligand field of the Cu(II) complexes in the homogeneous and heterogeneous phase strengthen this conclusion. Metal-uptake experiments with Cu(II) under non-competitive conditions, as reported previously,[16] have shown a maximum Cu(II) capacity of 64% at pH 5.7. This higher maximum uptake capacity for Cu(II) is due to the use of a large excess of Cu(II), *i.e.*, the use of 0.16 M $CuCl_2$ solutions instead of 0.011 M solutions, as used for the uptake experiments presented in this paper. In both cases full loading of the ion-exchange resin is not obtained, indicating that some ligands are not accessible at all for Cu(II).

The influence of Na_2H_2edta on the Cu(II) uptake of the ion exchanger is both pH and concentration dependent as can be seen in Figure 7A. At low Na_2H_2edta concentration (L_i:L_c is 1:0.5) a positive influence on the Cu(II) uptake is observed. At

(34) Lever, A. B. P. *Inorganic Electronic Spectroscopy*; Elsevier: Amsterdam, 1986.
(35) Linert, W.; Jameson, R. F.; Taha, A. *J. Chem. Soc. Dalton Trans.* **1993**, 3181

higher Na_2H_2edta concentrations, *i.e.*, L_i:L_c is 1:1 or 1:1.5, the Cu(II) uptake by pGMT-bimam decreases rapidly with increasing pH. The latter observation is most probably related to the pK_a values of Na_2H_2edta,[36] *i.e.*, at higher pH-values more H_2edta^{2-} molecules will be present as $Hedta^{3-}$ or $edta^{4-}$ which results in a better coordination ability toward the Cu(II) ions. At low Na_2H_2edta concentration, *i.e.*, L_i:L_c is 1:0.5, the increased uptake of Cu(II) seems small but is substantially larger than the experimental error of 6%. Most probably the Na_2H_2edta molecules act as Cu(II) carriers, thereby lowering the diffusion resistance and transporting more Cu(II) ions into the pores of the resin. H_4edta and nitrilotriacetate (nta) are known as additives in laundry detergents and might transport metal ions to the pores of the added zeolites. It is most likely that in the uptake experiments with a low Na_2H_2edta concentration as competitor in solution, a process analogous to the above-described mechanism takes place. Thus at low concentration of H_2edta^{2-}, the ligand bimam immobilized onto a polymer backbone is a stronger ligand than H_2edta^{2-}.

The influence of tartrate on the Cu(II) uptake of pGMT-bimam is shown in Figure 7B. For all concentrations of tartrate used, a substantial positive effect on the Cu(II) uptake by the resin is observed. Because of the poorer coordination ability of tartrate in comparison to ethylenediaminetetraacetate, tartrate might act as a carrier for Cu(II) ions even at high concentrations. EPR experiments performed with Cu(II)-loaded resins in the presence and absence of tartrate strengthen this hypothesis. For all concentrations of tartrate used in these experiments, bimam is a stronger coordinating ligand toward copper(II) ions than tartrate.

The use of three different diamines, *i.e.*, 1,2-diaminoethane, 1,3-diaminopropane and 1,4−diaminobutane, as competitors in solution did not have any influence on the Cu(II) uptake of the resin, *i.e.*, the resin retains its initial high Cu(II)-uptake capacity in the presence of 1,2-diaminoethane, 1,3-diaminopropane, and 1,4-diaminobutane. The Cu(II)-uptake capacities for pGMT-bimam found in the presence of these competing diamines are within the experimental error of the uptake capacities found for the blank. Even the use of a fivefold excess of diamine did not have any influence on the copper(II)-uptake capacity of pGMT-bimam. This can most probably be ascribed to the pK_a values of the diamines;[36] *i.e.*, all the diamines are hydronated in the pH range used for the uptake experiments, thereby considerably weakening the coordination ability of the diamine ligands toward metal ions.

(36) Lide, D. R., Frederikse, H. P. R., Eds. *Handbook of Chemistry and Physics*, 75th ed.; CRC Press: Boca Raton, FL, 1994−1995.

Concluding Remarks

The ligands bima and bimam both coordinate to copper(II) ions in a didentate fashion, as tridentate coordination is prevented for steric reasons. A possible driving force for the formation of the present complexes with the hydronation of the amine nitrogen donor might be the formation of an intramolecular chelate hydrogen bond between the amine nitrogen donor and the axial coordinated chloride anion.

Spectroscopic studies of the coordination compounds with bimam and bima in their relationship to chelation of Cu(II) ions on the ion-exchange resin pGMT-bimam showed that on the resin only 1:1 (Cu(II):bimam) complexes are formed. Although at low pH the aliphatic amine nitrogen donor of the ligand bimam is most probably hydronated, the Cu(II) uptake is still rather high. This can be explained by the fact that over the whole pH range tested, only the two imidazole nitrogens of the ligand take part in the coordination sphere around the Cu(II) ion.

The resin retains its initial high uptake capacity for Cu(II) in the presence of several different diamines as competing ligands in solution. When tartrate is used as a competitor, a positive effect on the Cu(II) uptake is observed, which is ascribed to the transport function of the tartrate molecules. For Na_2H_2edta as competitor in solution, both a pH effect and a concentration effect take place; *i.e.*, with increasing pH and increasing molar ratios of Na_2H_2edta the Cu(II) uptake by pGMT-bimam decreases rapidly.

Acknowledgment. Financial support by the European Union, allowing regular exchange of preliminary results with several European colleagues, under Contract ERBCHRXCT920014 is thankfully acknowledged. G.M.D. thanks the Commission of the European Union for support for a sabbatical visit through the fellowship Marie Curie (application No. 930258). We thank the Foundation for Chemical Research in the Netherlands (SON) for financial support.

Supporting Information Available: Labeled TME plots and further details of the structure determinations, including tables of atomic coordinates, bond lengths and angles, and thermal parameters for **A**, **B**, and **C** (11 pages). Ordering information is given on any current masthead page.

IC9513705